RSC Advances

PAPER

View Article Online
View Journal | View Issue

Cite this: *RSC Adv.*, 2015, **5**, 19853

Carbon dots based turn-on fluorescent probes for oxytetracycline hydrochloride sensing†

Xuting An, Shujuan Zhuo,* Ping Zhang and Changqing Zhu*

Received 16th December 2014
Accepted 11th February 2015

DOI: 10.1039/c4ra16456c

www.rsc.org/advances

In this paper, we have presented a facile, economic and green one-step hydrothermal synthesis route using tannic acid as carbon source to prepare water-soluble fluorescent carbon dots (CDs). The as-prepared CDs contain distinctive catechol groups on their surfaces, which have a special response toward Fe^{3+} ions. So the fluorescence emission of CDs gradually decreased with increasing Fe^{3+} ions. Such fluorescence responses can be used for well quantifying Fe^{3+} ions in the range of 0–5 μM with the detection limit of 24.4 nM. Most importantly, quenched fluorescence of CDs–Fe^{3+} could be recovered with the addition of oxytetracycline hydrochloride based on a competition mechanism, which provides a turn-on sensing strategy for oxytetracycline hydrochloride assay. The proposed sensing system has been successfully used for the assay of oxytetracycline hydrochloride in milk samples, indicating the practical potential.

1. Introduction

Oxytetracycline (OTC), as a kind of tetracycline antibiotic, is a broad-spectrum antibacterial agent. OTC possesses efficacy in respiratory and gastrointestinal therapies and has an amazing positive effect on the growth of livestock, so it is extensively used as a veterinary antibiotic and an animal growth promoter.[1,2] As a result, humans have an increased chance of a longterm intake of OTC. Whereas, abuse of OTC in farm animals can cause accumulation of antibiotics in food products, including meat, milk and chicken eggs,[3,4] which leads to a serious threat to human health.[5,6] Therefore, it is urgently needed to provide a simple and effective approach to detect the OTC in contaminated food products. However, the available conventional detection protocols do not meet the new demands.[7,8] The sensitivity and specificity of the traditional methods are not good enough for the detection of OTC in real samples,[9,10] and expensive instruments and tedious sample extraction procedures are usually required.[11–13] So it is great interest to explore new sensing strategy for OTC detection.

Fluorescent technique,[14,15] as a powerful tool, is superior due to its nondestructive nature, high sensitivity and wide dynamic ranges. High sensitivity is particularly important, considering the maximum residual value of OTC in drugs and human food is only 0.1 mg L^{-1} announced by world health organization.[16] Furthermore, the design of fluorescent probes for turn-on sensing of analytes is especially significant because it can effectively enhance sensing sensitivity by decreasing the background interference.[17]

Herein, we propose a novel strategy for carbon dots (CDs) fluorescence off/on modulation and demonstrate the corresponding application for turn-on sensing of OTC. The CDs are fabricated by on-step "synthesis modification integration" using tannic acid as precursor. So, the as-prepared CDs are directly functionalized by catechol groups (one of the most commonly used recognition sites for Fe^{3+}) in the particle synthesis. As a consequence, the added Fe^{3+} can lead to the assembly of the CDs based on the coordination binding between the Fe^{3+} and catechol groups on the CDs surface, which cause the almost complete quenching of the fluorescence emission. Interestingly, the fluorescence of the pre-quenched CDs is then gradually recovered in the presence of OTC due to the competition coordination (see Scheme 1). Such fluorescence response can be used for well quantifying OTC in the range of 0.1–2.7 μM with 22.8 nM detection limit, and has been successfully used for the assay of OTC in real milk samples. Due to simplicity and effectivity, it exhibits great promise as a practical platform for OTC sensing.

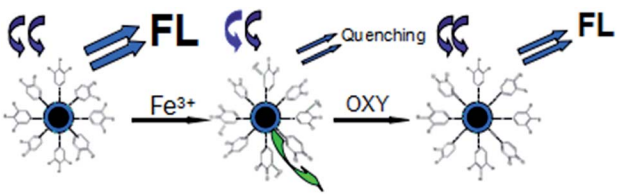

Scheme 1 Schematic illustration of CDs-based off/on fluorescence sensing principle.

Key Laboratory of Functional Molecular Solids, Ministry of Education, Anhui Key Laboratory of Chemo-Biosensing, College of Chemistry and Materials Science, Anhui Normal University, Wuhu, 241000, PR China. E-mail: sjzhuo@mail.ahnu.edu.cn; zhucq@mail.ahnu.edu.cn; Fax: +86 553 3869303; Tel: +86 553 3937137

† Electronic supplementary information (ESI) available: Figures concerning AFM, Raman spectrum, FT-IR, TEM, RLS, effect of pH, effect of time, effect of ionic strength and selectivity of the Fe^{3+} sensor. See DOI: 10.1039/c4ra16456c

2. Experimental section

2.1 Materials

Tannic acid and oxytetracycline hydrochloride were purchased from Sigma-Aldrich. Ethylenediaminetetraacetic acid (EDTA) disodium salt and $FeCl_3$ were obtained from Aladdin. Citric acid, Na_2HPO_4 and other routine chemicals were obtained from Shanghai Sinopharm Chemical Reagent Company. Other reagents were of analytical reagent grade and were used without further purification. Water used throughout was doubly deionized water.

2.2 Instruments and characterizations

The fluorescence and the absorption spectra were recorded with a Hitachi F-4600 fluorescence spectrophotometer and a Hitachi U-3010 spectrophotometer (Tokyo, Japan), respectively. Characterizations of transmission electron microscopy (TEM) were carried out on a Tecnai G^2 20 S-TWIN (FEI) operating at 200 kV. The sample for TEM measurements was prepared by the deposition of one drop of aqueous dispersion on a copper grid coated with thin films of carbon, and the solvent was removed by evaporation in air. Atom force microscopic (AFM) topography images were acquired from an Innova scanning probe microscope. Raman spectrum was collected on an HR 800 Raman spectroscopy (Jobin Yvon, France) equipped with a synapse CCD detector and a confocal Olympus microscope. The spectrograph uses 600 g mm^{-1} gratings and a 633 nm He–Ne laser. Fourier transform infrared (FT-IR) spectrum was measured from a KBr window on a PerkinElmer PE-983 FT-IR spectrophotometer. X-ray photoelectron spectroscopy (XPS) was performed by a thermoelectron instrument (Thermo-VG Scientific ESCALAB 250). The obtained spectra were calibrated with the reference to the 1s peak of carbon at 284.6 eV. All pH values were measured with a Model pHs-3C meter (Shanghai, China).

2.3 Preparation of fluorescent CDs

CDs were fabricated by a simple one-step hydrothermal route. Briefly, tannic acid (0.1035 g) and 40 mL H_2O were loaded into a teflon lined autoclave (50 mL capacity) and stirred for 10 min. The autoclave was sealed and maintained at 180 °C for 2 h, and then cooled to room temperature naturally. The obtained solution was dialyzed through a dialysis membrane (2000 MWCO). Then the products were collected by removing the large particles through centrifugation at 12 000 rpm for 15 min, and dried under vacuum for 48 h. Finally, the as-prepared CDs were dispersed in water for further use.

2.4 Detection of Fe^{3+}

Into a 5 mL volumetric flask was transferred 300 μL of citric acid–Na_2HPO_4 (pH = 7) buffer solution, 200 μL of CDs, followed by the addition of different amounts of Fe^{3+} ions. The mixture was diluted to 3 mL with water and thoroughly mixed. Then the fluorescence intensities were measured with the following settings of the spectrofluorimeter: excitation wavelength, $\lambda_{ex} = 440$ nm; emission wavelength, $\lambda_{em} = 507$ nm.

2.5 Treatment of the real samples

Milk samples were obtained from the local supermarket. The fresh milk samples was achieved by incubation in water at 55 °C for 30 min. Into a centrifuge tube was transferred 1.5 mL milk samples and 1.5 mL 0.1 mol L^{-1} Na_2EDTA–Mcllvaine buffer solution. After vibrating for 10 minutes, the mixture was centrifuged at a speed of 5000 rpm for 20 min. The supernatant was filtered with the rapid filter paper. Then 1 mL Na_2-EDTA–Mcllvaine buffer was added to the residue, again. The solution was extracted for 10 min by ultrasonic oscillation, and centrifugated at a speed of 5000 rpm for 10 min. Finally, the supernatant was filtrated with a 0.45 μM filtration membrane and for further use.

2.6 Procedures for OTC sensing

Into a 5 mL volumetric flask was transferred 300 μL of buffer solution, 200 μL of CDs, and an appropriate quantity of Fe^{3+} was added. Then, different amounts of OTC or real samples were added to the mixture. Finally, the mixture was thoroughly mixed and measured.

3. Results and discussion

The TEM image of the CDs is shown in Fig. 1a, demonstrating that the as-prepared CDs are mono-dispersed. Their size distribution ranges from 2 to 5.5 nm (Fig. 1b), and average diameter is 3.3 nm (80 random nanoparticles were accounted). The AFM image also indicates that the CDs are mostly spherical dots and well-separated (Fig. S1a†), which is in good agreement with the result of TEM. As described in Fig. S1b,† their height is about 3 nm.

Raman spectrum is measured to confirm the quality of the as-prepared CDs. The Raman spectrum of the CDs (Fig. S2†) displays two distinct peaks at 1343 and 1580 cm^{-1}, which are attributed to the D-band (sp^3) and G-band (sp^2), respectively. The D-band is associated with vibrations of carbon atoms with dangling bonds in the termination plane of disordered graphite or glassy carbon. The G-band is associated with the E_{2g} mode of graphite and is related to the vibration of sp^2-bonded carbon atoms in a two-dimensional hexagonal lattice.[18]

The surface structure and composition of the as-prepared CDs were then investigated. The FT-IR spectrum (Fig. S3†) of the CDs exhibits distinct absorption bands at 3300, 1700, 1400

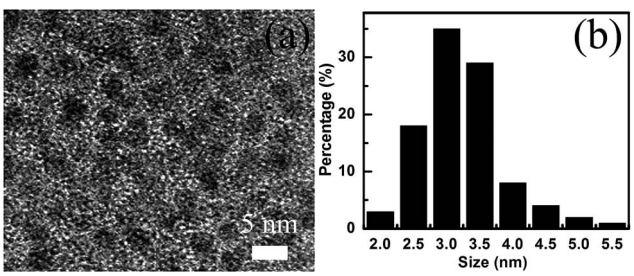

Fig. 1 (a) TEM image of as-prepared CDs; and (b) size distribution of the CDs.

and 1200 cm^{-1}, corresponding to the groups of OH, C=O, COOH and C–OH vibration mode,[19,20] respectively, imply the existence of large numbers of residual hydroxyl groups. In addition, the characteristic bands corresponding to the benzene skeleton vibrations can be observed at 1600 and 1450 cm^{-1},[21] and the benzene out-of-plane bending vibrations of C–H centered at 760 and 625 cm^{-1} are also appeared, indicating that benzene ring is present on the surface of the as-prepared CDs.

For a better insight, XPS measurements were performed. As shown in Fig. 2a, no peaks of other elements except C (282.2 eV) and O (533.9 eV) are observed. XPS analysis of the C1s spectrum (Fig. 2b) shows three peaks at 284.4, 285.9 and 288.5 eV, corresponding to C=C (45.55%), C–O (38.89%) and C=O (15.55%), respectively.[22] The O1s spectrum (Fig. 2c) consists of two peaks at 531.3 and 532.7 eV, which are ascribed to C=O (15.4%) and C–OH/C–O–C (84.6%).[23] These results indicate that catechol groups are successfully transferred from tannic acid molecules to the CDs surface during particle formation.

It is interesting to ask why the as-prepared CDs possess many catechol groups on the surfaces, namely, what is the formation mechanism of CDs. The possible explanation is as follows: the polymerisation and condensation of tannic acid gives rise to soluble polymers. When concentration of the polymers reaches a critical supersaturation point, burst nucleation takes place. The core of the CDs with graphite structure was formed by this process. Then, tannic acid that has no carbonization will self-polymerize to form polymer onto the graphitic core under high temperature and high pressure, suggesting that CDs are wrapped outside with the polymer that contains large numbers of catechol groups.[24]

To further explore the optical properties of as-synthesized CDs, the absorption and detailed fluorescence study by using different excitation wavelengths were carried out. The UV-vis absorption spectrum of CDs in water shows an absorption band at *ca.* 440 nm (Fig. 3a). In the inset to Fig. 3a, a photograph of the dispersed CDs illuminated under UV light (365 nm) is shown. The bright blue fluorescence of CDs is strong enough to be easily seen with the naked eye. Interestingly, as excitation wavelength increases from 380 to 480 nm, the fluorescence wavelength changes little and shows a strong peak at 507 nm with optimal excitation wavelength at 440 nm (Fig. 3b). This special feature may result from less surface defects and more uniform size of CDs.[25] The quantum yield of the CDs is estimated about 6.9% using rhodamine 101 as the reference, which is comparable to the value of previous reports.[26]

Typically, the phenolic hydroxyls would form complexes with Fe^{3+} ions due to coordination.[27] Thus, the as-prepared CDs are a potential candidate for Fe^{3+} sensing. As shown in Fig. S4,† the initial dispersed CDs aggregate together and form a large assembly, as Fe^{3+} is introduced to the CDs solution. To further demonstrate such assembly was caused by Fe^{3+} instead of drying on grid, resonance light scattering (RLS) was used to monitor the interaction. As described in Fig. S5,† the RLS signals become more and more strong with the increase of added Fe^{3+}. These *in situ* characterized data definitely demonstrate that the CDs assemble in solution with the assistance of Fe^{3+}, leading to enhanced light scattering signal. As one of the most essential metal ions in biological systems, Fe^{3+} plays crucial roles in many physiological and pathological processes.[28] Abnormal fluctuations (deficiency or overloading) of Fe^{3+} are the hallmarks of diseases.[29,30] Thus, the determination of Fe^{3+} is fundamentally important.[31,32]

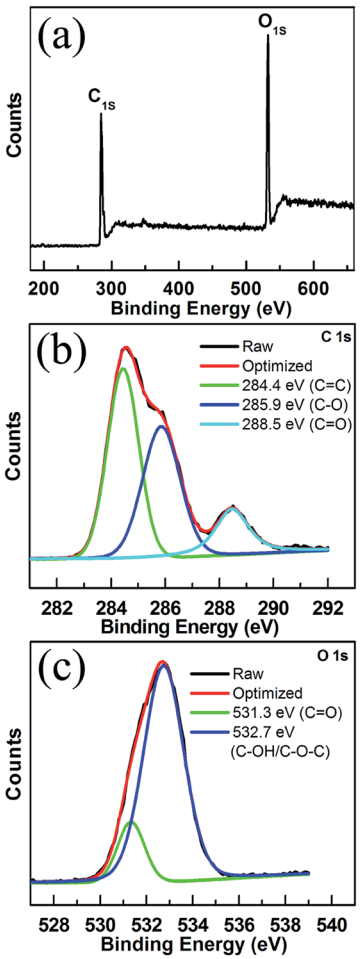

Fig. 2 (a) Entire XPS scanning spectrum of the CDs. XPS high-resolution survey scan of (b) C 1s and (c) O 1s of the CDs.

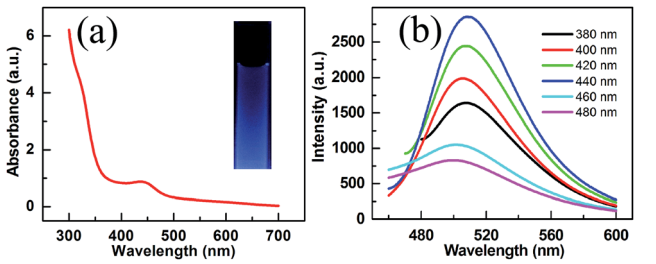

Fig. 3 (a) UV-vis absorption spectrum of the CDs dispersed in water. Inset: optical photograph of the CDs illuminated under UV light (365 nm). (b) Fluorescence spectra of the CDs at different excitation wavelengths.

Firstly, we investigate the influence of pH on the fluorescence of CDs. As shown in Fig. S6,† an increment of pH value from 2 to 7 leads to increased fluorescence intensity, whereas further increase to 11 results in a gradual decrease, demonstrating the fluorescence intensity of CDs strongly depends on the pH value. We speculated that the change of pH might result in electrostatic doping/charging of the CDs and shifts the Fermi level, which is associated with the process of protonation and deprotonation of the carboxyl groups on the surface of CDs.[33] Such observations are similar to those of CDs modified with hydroxyl and carboxylic/carbonyl moieties.[34] To obtain lower detection limits and better sensing performances for both Fe^{3+} and OTC, the pH 7.0 citric acid–Na_2HPO_4 buffer system was selected in this work. The reaction time also affects the quenching effects. As described in Fig. S7,† the interactions can reach the balance at 20 min. As a consequence, 20 min of reaction time was appropriate for the sensing. Then the effects of different concentrations of sodium chloride on the fluorescence response of the system were evaluated. As shown in Fig. S8,† the change of ionic strength had no effect on the fluorescence intensity of the system, demonstrating high stability of the sensing system.

Under the conditions discussed above, the linear response range of the sensing system was measured. As shown in Fig. 4a, the fluorescence intensities of the CDs are highly sensitive to Fe^{3+} and decrease as the concentration of the analyte is increased. There is a good linear relationship ($R^2 = 0.992$) between the F_0/F and the concentrations of Fe^{3+} in the range from 0 to 5 μM (Fig. 4b) with a detection limit of 24.4 nM (signal-to-noise ratio of 3), which is lower than other previously reported values,[24,35] indicating the higher sensitivity of the present sensing system, where F_0 and F are the fluorescence intensities of CDs without and with Fe^{3+}.

Interference test was carried out. It can be seen that those tested metal ions such as Co^{2+}, Cu^{2+}, Al^{3+}, Cr^{3+} and so on are scarcely interfered (Fig. S9†), indicating the high selectivity.

In general, oxytetracycline hydrochloride, containing phenolic hydroxyl and enolic hydroxyl, could be chelate with Fe^{3+}, which might reduce the influence of Fe^{3+} to the CDs fluorescence, and cause the recovery of fluorescence intensity of pre-quenched CDs. Thus, the present CDs–Fe^{3+} complex might

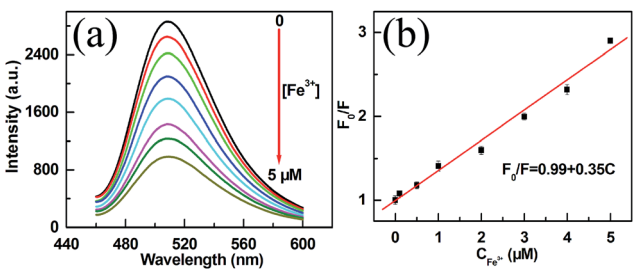

Fig. 4 (a) Fluorescence spectra of the CDs at various Fe^{3+} concentrations. (b) Linear plots of the ratio of intensity against the concentration of Fe^{3+}. F_0 and F are fluorescence intensities of the CDs in the absence and presence of the analytes, respectively. The error bars represent the standard deviation of three measurements.

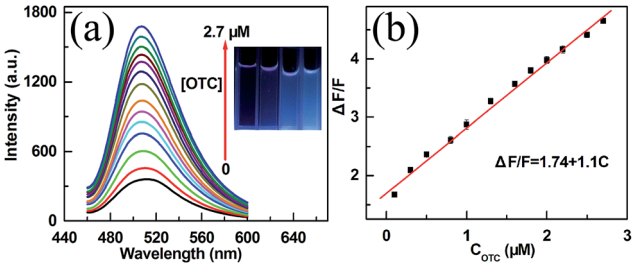

Fig. 5 (a) Evolutions of fluorescence spectra of the CDs–Fe^{3+} system with increasing amounts of OTC. Inset: optical photograph of the CDs–Fe^{3+} system with different concentrations of OTC illuminated under UV light (365 nm). (b) Linear plots of the $\Delta F/F$ against the concentration of OTC. ΔF and F are recovered fluorescence intensity of CDs–Fe^{3+} system in the presence of OTC and fluorescence intensity of the CDs–Fe^{3+}, respectively. The error bars represent the standard deviation of three measurements.

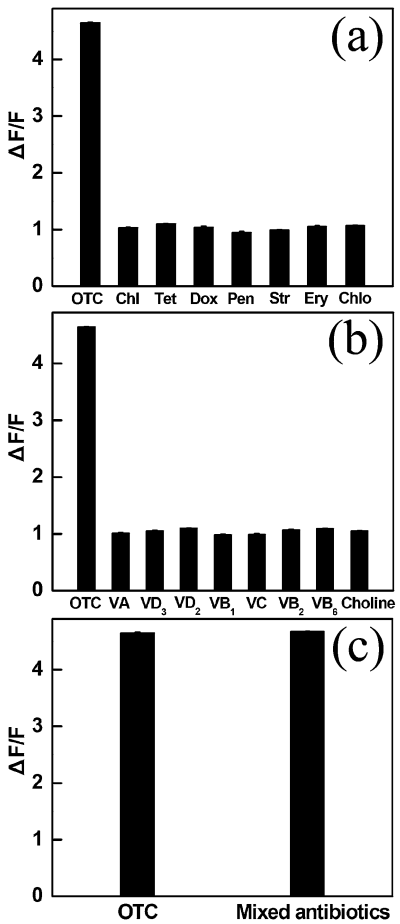

Fig. 6 (a) The CDs–Fe^{3+} system toward various potential interfering antibiotics. The concentrations of various antibiotics (from left to right) are 2.7, 165, 105, 180, 300, 300, 300 and 300 μM, respectively. (b) Fluorescence responses of the CDs–Fe^{3+} system toward various vitamins. The concentrations of all vitamins are 1.5 mM. (c) Fluorescence responses of the CDs–Fe^{3+} system toward mixed antibiotics. The mixture of antibiotics include OTC (2.7 μM), chlortetracycline (165 μM), doxycycline (180 μM), tetracycline (105 μM), and 300 μM penicillin, streptomycin, erythromycin, chloramphenicol.

Table 1 Determination results of OTC in diluted milk samples ($n = 4$)

Sample	Content of OTC/μM	OTC added/μM	OTC found/μM	Recovery (%)
1	0.13 ± 0.02	2	2.01 ± 0.06	94.0 ± 0.31
2	0.06 ± 0.03	2	1.99 ± 0.24	96.5 ± 1.15
3	0.06 ± 0.01	2	1.91 ± 0.08	92.5 ± 2.52
4	0.11 ± 0.03	2	2.14 ± 0.33	101.5 ± 4.1
5	0.05 ± 0.01	2	2.11 ± 0.12	103.0 ± 5.2

be a potential candidate for turn-on OTC sensing. As we expected, the fluorescence intensity of quenched CDs is gradually recovered with the increment of OTC (Fig. 5a), and can be visually observed by naked eyes (inset of Fig. 5a). It can be seen from Fig. 5b, there is a good linear relationship ($R = 0.997$) between $\Delta F/F$ and the concentration of OTC in the range from 0.1 to 2.7 μM with a 22.8 nM detection limit, where ΔF is the recovered fluorescence intensity of CDs–Fe^{3+} system in the presence of OTC and F is the fluorescence intensity of the CDs–Fe^{3+}.

Selectivity is a critical parameter to evaluate the performance of a fluorescent chemosensor. We first studied the fluorescence responses of the CDs–Fe^{3+} toward the potential interfering substances coexisting in milk sample, including structurally similar tetracycline group antibiotics and primary vitamins. As shown in Fig. 6a, other seven kinds of antibiotics, including penicillin (Pen), streptomycin (Str), erythromycin (Ery), chloramphenicol (Chl), tetracycline (Tet), doxycycline (Dox) and chlortetracycline (Chio) have very little effects on the CDs–Fe^{3+} system fluorescence. Then the influence of various primary vitamins was studied. As can be seen from Fig. 6b, these tested vitamins are scarcely interfered. The exclusive response of OTC probably results from the fact that the OTC contains more phenol hydroxyl, enol hydroxyl and carbonyl, which strengthens the coordination ability. However, the exact mechanism is not clear and needs further study. It should be noted here that the OTC can still be detected in the presence of the mixture of all possible coexistence antibiotics (Fig. 6c).

To further investigate the potential practical applications of this method, the sensing of OTC in real milk samples was performed. The results of recovery tests from 92.5 to 103% are satisfying (Table 1). The above results fully indicated the practicability and reliability of the proposed sensing platform for OTC detection in real samples.

4. Conclusions

In summary, a novel and well-designed turn-on sensing strategy has been proposed for OTC assay, by using CDs–Fe^{3+} assembly as fluorescence reporters. The turn-on fluorescence signal output is expected to dramatically enhance the sensitivity because of low background interference, which is especially desirable for the OTC due to the maximum residual value in food is very low. By means of the platform of CDs-metal ions system and the rational design of the particle surface chemistry, it is promising to develop a general turn-on sensing strategy for other analytes.

Acknowledgements

This work is financially supported by the National Natural Science Foundation of China (nos 21175003, 21375003 and 21303003).

Notes and references

1 C. H. Kim, L. P. Lee, J. R. Min, M. W. Lim and S. H. Jeong, *Biosens. Bioelectron.*, 2014, **51**, 426–430.
2 D. Y. Zheng, X. L. Zhu, X. J. Zhu, B. Bo, Y. M. Yin and G. X. Li, *Analyst*, 2013, **138**, 1886–1890.
3 A. L. Cinquina, F. Longo, G. Anastasi, L. Giannetti and R. Cozzani, *J. Chromatogr. A*, 2003, **987**, 227–233.
4 K. DeWasch, L. Okerman, S. Croubels, H. DeBrabander, J. VanHoof and P. DeBacker, *Analyst*, 1998, **123**, 2737–2741.
5 H. Hou, X. J. Bai, C. Y. Xing, N. Y. Gu, B. L. Zhang and J. L. Tang, *Anal. Chem.*, 2013, **85**, 2010–2014.
6 J. Y. Sun, T. Gan, W. Meng, Z. X. Shi, Z. W. Zhang and Y. M. Liu, *Anal. Lett.*, 2015, **48**, 100–115.
7 N. Link, W. Weber and M. J. Fussenegger, *Biotechnology*, 2007, **128**, 668–680.
8 D. Vega, L. Aguei, A. Gonzalez-Cortes, P. Yanez-Sedeno and J. M. Pingarron, *Anal. Bioanal. Chem.*, 2007, **389**, 951–958.
9 C. C. Weber, N. Link, C. Fux, A. H. Zisch, W. Weber and M. Fussenegger, *Biotechnol. Bioeng.*, 2005, **89**, 9–17.
10 Y. S. Kim, J. H. Kim, I. A. Kim, S. J. Lee, J. Jurng and M. B. Gu, *Biosens. Bioelectron.*, 2010, **26**, 1644–1649.
11 L. Norambuena, N. Gras and S. Contreras, *Mar. Pollut. Bull.*, 2013, **73**, 154–160.
12 I. Pérez-Silva, J. A. Rodríguez, M. T. Ramírez-Silva and M. E. Páez-Hernández, *Anal. Chim. Acta*, 2012, **718**, 42–46.
13 G. Kahsay, F. Shraim, P. Villatte, J. Rotger, C. Cassus-Coussíre, A. Van Schepdael, J. Hoogmartens and E. Adams, *J. Pharm. Biomed. Anal.*, 2013, **75**, 199–206.
14 W. L. Wei, C. Xu, J. S. Ren, B. L. Xu and X. G. Qu, *Chem. Commun.*, 2012, **48**, 1284–1286.
15 K. Škrášková, L. H. M. L. M. Santos, D. Šatínský, A. Pena, M. C. B. S. M. Montenegro, P. Solich and L. Nováková, *J. Chromatogr. B: Anal. Technol. Biomed. Life Sci.*, 2013, **927**, 201–208.
16 W. Xu, S. Liu, J. H. Yu, M. Cui, J. Li, Y. N. Guo, H. Z. Wang and J. D. Huang, *RSC Adv.*, 2014, **4**, 10273–10279.
17 Y. S. Xia, J. J. Wang, Y. Z. Zhang, L. Song, J. J. Ye, G. Yang and K. H. Tan, *Nanoscale*, 2012, **4**, 5954–5959.
18 B. J. Wang, S. J. Zhuo, L. Y. Chen and Y. J. Zhang, *Spectrochim. Acta, Part A*, 2014, **131**, 384–387.

19 M. J. Bojdys, J.-O. Muller, M. Antonietti and A. Thomas, *Chem.–Eur. J.*, 2008, **14**, 8177–8182.
20 W. Shi, Q. Wang, Y. Long, Z. Cheng and S. Chen, *Chem. Commun.*, 2011, **47**, 6695–6697.
21 J. G. Wang, F. L. Cao, Z. F. Bian, Z. F. Bian, M. K. H. Leung and H. X. Li, *Nanoscale*, 2014, **6**, 897–902.
22 S. Liu, J. Tian, L. Wang, Y. Luo, J. Zhai and X. Sun, *J. Mater. Chem.*, 2011, **21**, 11726–11729.
23 S. Liu, J. Tian, L. Wang, Y. Luo, W. Lu and X. Sun, *Biosens. Bioelectron.*, 2011, **26**, 4491–4496.
24 K. G. Qu, J. S. Wang, J. S. Ren and X. G. Qu, *Chem.–Eur. J.*, 2013, **19**, 7243–7249.
25 M. M. Xie, Y. J. Su, X. N. Lu, Y. Z. Zhang, Z. Yang and Y. F. Zhang, *Mater. Lett.*, 2013, **93**, 161–164.
26 W. B. Lu, X. Y. Qin, S. Liu, G. H. Chang, Y. W. Zhang, Y. L. Luo, A. M. Asiri, A. O. Al-Youbi and X. P. Sun, *Anal. Chem.*, 2012, **84**, 5351–5357.
27 H. B. Xu, S. H. Zhou, L. L. Xiao, H. H. Wang, S. Z. Li and Q. H. Yuan, *J. Mater. Chem. C*, 2015, **3**, 291–297.
28 G. Alberti, G. Emma, R. Colleoni, M. Pesavento, V. M. Nurchib and R. Biesuza, *Analyst*, 2014, **139**, 3940–3948.
29 C. Brugnara, *Clin. Chem.*, 2003, **49**, 1573–1578.
30 N. Narayanaswamy and T. Govindaraju, *Sens. Actuators, B*, 2012, **161**, 304–310.
31 S. H. Li, Y. C. Li, J. Cao, J. Zhu, L. Z. Fan and X. H. Li, *Anal. Chem.*, 2014, **86**, 10201–10207.
32 R. Vikneswaran, S. Ramesh and R. Yahya, *Mater. Lett.*, 2014, **136**, 179–182.
33 S. Gómez-de Pedro, A. Salinas-Castillo, M. Ariza-Avidad, A. Lapresta-Fernández, C. Sánchez-González, C. S. Martínez-Cisneros, M. Puyol, L. F. Capitan-Vallveyb and J. Alonso-Chamarroa, *Nanoscale*, 2014, **6**, 6018–6024.
34 Q. Zhao, Z. Zhang, B. Huang, J. Peng, M. Zhang and D. Pang, *Chem. Commun.*, 2008, **41**, 5116–5118.
35 F. Nie, Z. Wang and Y. He, *Chin. J. Anal. Chem.*, 2000, **28**, 1516–1518.